AIAA 79-0006R

Velocity Space Description of Certain Turbulent Free Shear Flow Characteristics

R. J. Bywater*
The Aerospace Corporation, El Segundo, Calif.

Solutions of a statistical model of turbulence are presented for the transverse turbulence field of a two-dimensional shear layer. They are obtained by direct numerical solution for the velocity distribution function upon which the model is based without the use of approximate moment methods. The result is a velocity space description of the shear flow without the need for empirical turbulent transport coefficients. The transverse component of the turbulence energy is obtained by an ensemble average over the solution and found to be in agreement with data. Due to the ability to form all higher order correlations from the distribution function, the derivation of an eddy diffusivity from the solution is demonstrated.

Introduction

MANY approaches to turbulence modeling have been advanced in recent years with a great deal of current effort being expended on such closure techniques as Reynolds stress models.[1] A large class of the current turbulence models of this type are based on the determination of the various one-point correlations for the velocity field as well as temperature and species. The present work is concerned with an alternate approach to turbulence modeling which seeks to describe the statistical nature of the velocity field.[2-5] This is accomplished by a kinetic theory approach which uses a probability density function (pdf) to characterize the velocity fluctuations responsible for most engineering observables that distinguish the turbulent shear flow from its laminar counterpart. The result is elimination of the need for modeling higher order correlations introduced by the use of averaged conservation equations. The statistical closure invoked by the present approach results in a governing equation for the pdf whose solution yields all order one-point correlations of engineering interest.

Past solutions to the present statistical model developed by Chung[2-5] have generally considered simple one-dimensional geometries employing the approximate moment method of Liu and Lees.[2] The reason for those two simplifications was to demonstrate the ability of the statistical model to inherently describe certain basic physical phenomena of chemically reacting turbulent shear flows. Two primary results of those studies were the descriptions of turbulent shear flow structure without the use of turbulent transport coefficients (eddy viscosities) and the broad turbulent diffusion flame known to exist even in the limit of fast reactions. The one exception to the use of this solution technique was the work of Hong[6] in which a Green's function was used to integrate the governing equation for the pdf directly. However, as noted by Hong, this approach involves certain approximations to the initial conditions and the governing equation.

Therefore, since these previous studies have demonstrated the inherent advantages of this simplified kinetic theory approach to turbulence modeling, investigations of more complex problems utilizing direct numerical solutions of the governing equations are warranted. The present work takes the first step in that direction by demonstrating for the first time direct numerical solutions of the present statistical model in velocity space. The problem chosen for this initial calculation is the two-dimensional free shear layer (see Fig. 1). The simplicity of this geometry as compared with the types of complicated three-dimensional flowfields being considered in various branches of fluid mechanics permits a substantial reduction in the required computational effort. It does, however, represent a significant advance beyond the one-dimensional geometries amenable to the above-mentioned moment method. With the main emphasis on exploring the impact of velocity space solutions on the description of turbulent structure, an added simplification is introduced in this initial study. Calculations are performed only for the normal component of the turbulence field which governs the mixing phenomena in the shear layer. This allows the use of a reduced form of the governing equation for the pdf, thereby simplifying the computational procedure while maintaining the important physics. Data comparisons will be made to demonstrate the general agreement of the solutions with typical shear layer behavior. Emphasis will be on a velocity space explanation for that behavior.

Presented as Paper 79-0006 at the AIAA 17th Aerospace Sciences Meeting, New Orleans, La., Jan. 15-17, 1979; submitted June 11, 1979; revision received Jan. 6, 1981.

*Engineering Specialist, Fluid Mechanics Department. Member AIAA.

General Theory

In this section the kinetic theory approach to turbulence modeling is outlined. The concepts surrounding the use of the pdf are defined mathematically, and the governing equation is presented. A generalized moment equation is derived from the governing equation to facilitate later application of the reduction technique employed to obtain the solutions.

Governing Kinetic Equation

The methodology of the kinetic theory approach proceeds by definition of a pdf for the fluctuating velocity field in analogy with the pdf for molecular fluctuating velocities. The motivation for this approach is the recognition that the one-point correlations required for engineering calculations can be based on, and therefore imply, the existence of a probability density function f (t,x,u). Thus, fdu gives the probability of a fluid element at time t and location x having its instantaneous velocity in the range u to $u+du$. It is related to the correlations that are the dependent variables for moment closure methods through the ensemble average.

$$\langle Q(u)\rangle = \int_{-\infty}^{\infty}\int_{-\infty}^{\infty}\int_{-\infty}^{\infty} Q(u)f(t,x,u)\,du \qquad (1)$$

Insertion of specific values for Q into Eq. (1) results in specific velocity moments.

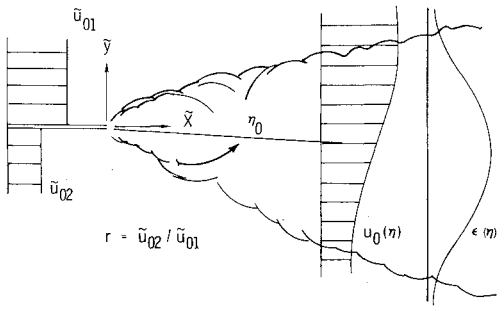

Fig. 1 The two-dimensional free shear layer.

$$\langle u_i \rangle \quad \equiv \text{mean velocity}$$

$$\langle U_i U_j \rangle \quad \equiv \text{Reynolds stress} \quad i \neq j$$

$$\langle U_k U_k \rangle \quad \equiv \text{turbulent kinetic energy} \tag{2}$$

where $U \equiv u - \langle u \rangle$. The subscripts i, j, k are used to denote Cartesian coordinates where U_1, U_2, U_3 (or $\tilde{U}$, $\tilde{V}$, $\tilde{W}$) correspond to the velocity components in the x_1, x_2, x_3 (or $\tilde{x}$, $\tilde{y}$, $\tilde{z}$) directions. Figure 1 illustrates the flowfield geometry in this system. It is seen from Eqs. (1) and (2) that if a solution for f can be obtained, then all higher order moments are immediately available. It may further be surmised that modeling efforts can be better focused when concentration is on the single function f as opposed to attempts at individually modeling the behavior of various velocity correlations.

The derivation of the governing equation for $f(t,x,u)$ is analogous to the derivation of the Boltzmann equation in the kinetic theory of gases. A time-dependent conservation equation for f is developed in six-dimensional (x,u) space. This equation contains an operator that governs the variation of $f(t,x,u)$ due to interactions between the velocity fluctuations similar to the manner in which the molecular velocity distribution varies as a result of molecular interactions expressed by the collision operator of the Boltzmann equation.

The turbulence interaction operator is derived from a stochastic model of the velocity fluctuations. The details of applying this methodology to arrive at the following governing equation for f as applied to free shear layers can be found in the literature.[2-4]

$$\frac{\partial f}{\partial t} + u_j \frac{\partial f}{\partial x_j} = \beta \left\{ (1+D) \frac{\partial (U_j f)}{\partial U_j} + \frac{\langle U_k U_k \rangle}{3} \frac{\partial^2 f}{\partial U_j \partial U_j} \right\} \tag{3}$$

In Eq. (3), β is the rate at which the large eddies approach statistical equilibrium given by

$$\beta = A \langle U_k U_k \rangle^{1/2} / 2\Lambda \tag{4}$$

The only restriction placed on A in past studies was that it be of order one. The Λ is related to the macrolength scale of the large eddies, while D is the ratio of the characteristic dissipation rate to the equilibration rate β. Specific values for these quantities will be given in conjunction with the parameters used to specify the geometry of the system.

As stated earlier, the intent of the present work is to develop numerical solutions to Eq. (3) in velocity space. In the following sections, Eq. (3) will be put in a more convenient form for this purpose while simplifying it to the normal component of the turbulence field for the two-dimensional geometry of interest.

Generalized Moment Equation for $Q(\tilde{U}, \tilde{W})$

For the two-dimensional (physical space) problem to be considered, the dimensionality of the pdf can be reduced by the following technique used in molecular kinetic theory.[7] By integrating over $\tilde{U}$ and $\tilde{W}$, only the dependence of f on the velocity coordinate $\tilde{V}$, which is responsible for the mixing phenomena, will be retained. Thus, a generalized moment equation for a generic function $Q(\tilde{U}, \tilde{W})$ is obtained by multiplying Eq. (3) by Q and integrating over all $\tilde{U}$ and $\tilde{W}$ as follows:

$$\begin{aligned} &\frac{\partial}{\partial t} \int\int Q f \mathrm{d}\tilde{U} \mathrm{d}\tilde{W} - \frac{\partial u_{0k}}{\partial t} \int\int \frac{\partial f}{\partial U_k} Q \mathrm{d}\tilde{U} \mathrm{d}\tilde{W} \\ &+ \frac{\partial}{\partial x_k} \int\int (u_{0k} + U_k) f Q \mathrm{d}\tilde{U} \mathrm{d}\tilde{W} \\ &- \frac{\partial u_{0m}}{\partial x_k} \int\int (u_{0k} + U_k) Q \frac{\partial f}{\partial U_m} \mathrm{d}\tilde{U} \mathrm{d}\tilde{W} \\ &= \beta (1+D) \int\int Q \frac{\partial (U_k f)}{\partial U_k} \mathrm{d}\tilde{U} \mathrm{d}\tilde{W} \\ &+ \frac{\beta \langle U_k U_k \rangle}{3} \int\int \frac{\partial^2 f}{\partial U_m \partial U_m} Q \mathrm{d}\tilde{U} \mathrm{d}\tilde{W} \end{aligned} \tag{5}$$

where the limits of integration are $(-\infty, \infty)$. By choosing appropriate values of Q, a set of equations can be derived for partial integrals over f which govern the turbulence flowfield of a two-dimensional free shear flow. In deriving Eq. (5) a transformation from instantaneous velocity coordinates (t,x,u) to relative velocity coordinates (t,x,U) was introduced, where u_{0i} (or $\tilde{u}_0, \tilde{v}_0, \tilde{w}_0$) $\equiv \langle u_i \rangle$.

Two-Dimensional Free Shear Layer

The two-dimensional free shear layer (Fig. 1) was chosen for this initial calculation because it is a simple geometry, yet incorporates the two-dimensional convection effects not present in one-dimensional problems such as homologous or Couette flows. It also provides the basis for studies of reacting flows such as diffusion flames including the effects of shear.

Mathematical Formulation

As stated in the Introduction, in order to clarify the nature of velocity space calculations, the problem will be simplified by considering only the V-component turbulence velocity field. Because this component is responsible for the turbulent transport across the shear layer, it will be possible to explain the major features of turbulent transport on the basis of the statistically nonequilibrium velocity fluctuations. The pdf $\tilde{f}_{\tilde{V}}(t,x,\tilde{V})$ for the normal velocity field is related to f by the following expression.

$$\tilde{f}_{\tilde{V}}(t,x,\tilde{V}) = \int_{-\infty}^{\infty} \int_{-\infty}^{\infty} f(t,x,\tilde{U},\tilde{V},\tilde{W}) \mathrm{d}\tilde{U} \mathrm{d}\tilde{W} \tag{6}$$

The steady-state equation for $\tilde{f}_{\tilde{V}}$ for the present geometry is obtained from Eq. (5) by setting $Q = 1$, $\partial/\partial t = 0$, and invoking the thin shear layer approximations.

$$\tilde{u}_0 \frac{\partial \tilde{f}_{\tilde{V}}}{\partial \tilde{x}} + (\tilde{v}_0 + \tilde{V}) \frac{\partial \tilde{f}_{\tilde{V}}}{\partial \tilde{y}} = \beta \left[(1+D) \frac{\partial (\tilde{V} \tilde{f}_{\tilde{V}})}{\partial \tilde{V}} + \frac{\langle U_k U_k \rangle}{3} \frac{\partial^2 \tilde{f}_{\tilde{V}}}{\partial \tilde{V}^2} \right] \tag{7}$$

Before proceeding with the solution of Eq. (7), it will be transformed into standard shear layer spatial coordinates followed by a velocity space transformation.

Coordinate Transformations

The commonly used free shear layer coordinate $\eta = \sigma \tilde{y}/\tilde{x}$ and a shift in the velocity variable are used to transform Eq.

(7) from $(\tilde{x},\tilde{y},\tilde{V})$ to (x,η,V), resulting in

$$u_0 x\frac{\partial f_V}{\partial x}+V\frac{\partial f_V}{\partial \eta}$$
$$=B\epsilon^{1/2}\left\{(1+D)\frac{\partial}{\partial V}[(V+u_0\eta-v_0)f_V]+\frac{\epsilon}{3}\frac{\partial^2 f_V}{\partial V^2}\right\} \quad (8)$$

where the following relations have been used to obtain Eq. (8):

$$u_0=\tilde{u}_0/(u_{01}\epsilon_0^{1/2}),\quad \epsilon=\hat{\epsilon}/\epsilon_0,\quad f_V=\left(\frac{u_{01}\epsilon_0^{1/2}}{\sigma}\right)\hat{f}_V$$
$$v_0=\sigma\tilde{v}_0/(u_{01}\epsilon_0^{1/2}),\quad \hat{\epsilon}=\frac{\sigma^2\langle U_k U_k\rangle}{u_{01}^2},\quad V=\hat{V}+v_0-u_0\eta$$
$$\epsilon_0=\hat{\epsilon}(\eta=\eta_0),\quad \hat{V}=\frac{\sigma\tilde{V}}{u_{01}\epsilon_0^{1/2}},\quad x=\tilde{x}/L \quad (9)$$

where u_{01} and u_{02} are the velocities of the high- and low-speed streams, respectively, with the ratio denoted by $r=u_{02}/u_{01}$. The coordinate η_0 denotes the dividing streamline. Results to be presented in the following sections will be in terms of $\hat{V}$, while V is introduced for computational convenience. The term L is a scale length for the x coordinate related to the virtual origin[8] location whose value does not actually enter the calculations. The term B is defined, as a result of the transformation, to be

$$B=\frac{Ax}{2\sigma(\Lambda/L)} \quad (10)$$

Previous studies[9] have shown Λ to be proportional to the width of the mixing layer and could be specified as such while performing the solution. However, in keeping with the spirit of these simplified calculations, it will be input as being linearly proportional to x as determined experimentally.[8]

$$\Lambda/L=\ell_s x \quad (11)$$

Using Eq. (11), Eq. (10) becomes

$$B=A/2\sigma\ell_s \quad (12)$$

B is therefore a constant determined by the geometry of the flow.

Companion equations for Eq. (8) can be obtained from Eq. (5) with other choices for Q, which would then determine the complete flowfield including u_0, v_0, and ϵ. However, for this investigation of the transverse velocity field, certain mean flow information will be supplied in place of those additional equations from known solutions for free shear layers. The u_0 is given by[8,10]

$$u_0=\left(\frac{1+r}{2\epsilon_0^{1/2}}\right)\left[1+\left(\frac{1-r}{1+r}\right)\mathrm{erf}(\eta-\eta_0)\right] \quad (13)$$

The term v_0 is obtained by integration of the continuity equation with an experimentally determined constant of integration.[8] The turbulence energy profile is taken from Ref. 6 for the present geometry.

$$\epsilon(\eta)=\exp(-1.4|\eta|^{1.8}) \quad (14)$$

It is emphasized that Eqs. (13) and (14) are used to reduce the computational effort of solving a set of simultaneous equations to that of a single equation, and are not required inputs to the model. From previous studies[6,11] with the present model, D was found to be $\approx 1/3$ while A has been determined to be ≈ 3.0. Experimental values of 20 and 50 for σ and 0.044 and 0.016 for ℓ_s correspond to values of 0.3 and 0.6, respectively, for r, the velocity ratio of the two streams. These values of r characterize the two sets of data with which comparisons will be made. With Eq. (8) completely determined, its solution for the V component turbulence field of a two-stream mixing layer will be discussed in the following section.

Solution of Eq. (8)

Equation (8) is solved by marching in the streamwise coordinate. It was found in doing so that the solution relaxes to one which depends only on η and V. This might have been expected in view of known similarity solutions for the mixing layer in the mean. An inspection of Eq. (8) also reveals that if the x derivative is neglected, no terms exist which violate the assumption that f_V is independent of x. Before a detailed discussion of the solution technique, the boundary conditions will be determined.

Boundary Conditions

As discussed earlier, once the pdf is obtained, more details of the flowfield structure can be gathered beyond that which is available at the mean level through correlations. Therefore, it might be expected that the specification of boundary conditions on f_V entails greater detail. A brief discussion of this aspect of the problem will be given here.

Besides the apparent need for additional boundary conditions resulting from the added velocity space coordinates, there are certain conceptual differences in specifying boundary conditions for a pdf as compared to mean quantities. Thought must be given to the statistical behavior of the fluid elements as boundaries are approached. The analogy with the kinetic theory of gases provides the framework for this development.

It is first observed that Eq. (8) is first order in η and second order in V. Conventional methods utilizing transport coefficients impart a second-order character in η to the mean equations by assuming gradient transport. In that case, there is clearly a need for two boundary conditions[10] in η reflecting the influence of the two bounding streams. Physically, it is expected that both streams should impact the mechanics occurring within the mixing layer. However, the imposition of two η boundary conditions upon Eq. (8) would seem to overspecify the problem. The solution to this dilemma lies in the velocity space character of the problem and is paralleled by endeavors to solve the Boltzmann equation for such two-dimensional geometries. Introduction of the velocity coordinate V alters the nature of assigning boundary conditions from the one-dimensional η-interval for which the boundary consists of the two end points to the two-dimensional η-V plane for which the boundary is now a contour (see Fig. 2). Selection of the correct boundary contour is made by analogy

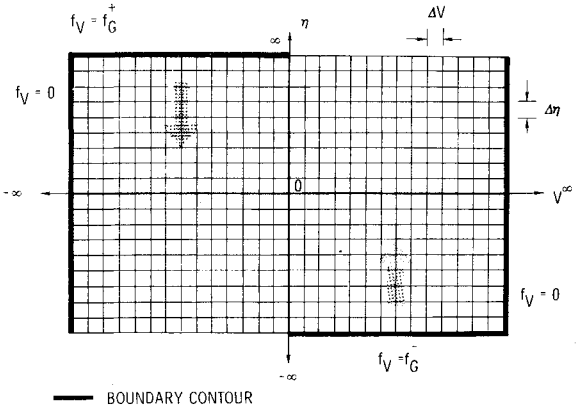

Fig. 2 Computational η-V domain.

with the physics of molecular-surface interactions.[12] For example, in the Couette flow of rarefied gases, molecules issue from the parallel plates normal to the direction of flow bearing the characteristics of their respective originating boundaries. The pdf's for this class of boundary molecules are therefore known and provide the boundary conditions for such a calculation. The other class of boundary molecules strikes the boundaries. Their properties are not known, a priori, and must be determined from the solution. Definition of these boundary molecules in terms of the independent variables establishes the boundary contour upon which values for the pdf must be specified. Analogously, for the present problem the turbulence pdf is specified for the fluid elements entrained from the bounding streams. Mathematically, these entrained fluid elements correspond to values of η for which the freestream properties are attained and values of V at those boundaries directed inward toward the mixing layer. These conditions, together with the requirement that the pdf approach zero as V tends to infinity in both directions, suffice to define the boundary contour of Fig. 2 as well as the following set of boundary conditions.

$$\begin{aligned} &\eta\to\infty,\ V<0 && f_V(\eta,V)\to f_G^+(V)\\ &\eta\to-\infty,\ V>0 && f_V(\eta,V)\to f_G^-(V)\\ &V\to\pm\infty,\ \text{all } \eta && f_V(\eta,V)\to 0 \end{aligned} \tag{15}$$

where f_G^+ and f_G^- characterize the turbulence in the streams at $\pm\infty$, respectively. The turbulence in both streams is taken as homogeneous and represented by a Gaussian pdf. Equivalently, f_G^+ and f_G^- represent solutions to Eq. (8) in the absence of η-gradients reflecting a balance in the V-fluctuations between the dissipation and the exchange with the U and W components. The $f_G^\pm$ is given explicitly by the following expression:

$$f_G^\pm = \frac{1}{\sqrt{2\pi\epsilon^\pm/[3(1+D)]}}\exp\left[\frac{-(V-v_0+u_0\eta)^2}{2\epsilon^\pm/3(1+D)}\right] \tag{16}$$

where $\epsilon^\pm$ represents the nondimensional turbulence energy in the two streams. An initial condition must also be provided in order to start the marching scheme used to calculate f_V. Therefore, f_V is initially specified to be Gaussian for all η in the form of Eq. (16) with a small and everywhere constant turbulence energy ϵ.

Equation (15) is consistent with the mathematical character of the convective derivative $V(\partial f_V/\partial\eta)$ in Eq. (8) which requires that upstream boundary conditions be specified and information propagate in the direction of the arrows in Fig. 2, as determined by the sign of V. With this interpretation, Fig. 2 can be viewed as depicting a two-dimensional reversed flow in the positive and negative η directions with a dividing streamline at $V=0$. The split boundary contour is therefore seen to provide for a consistent set of boundary conditions without overspecification.

Solution Procedure

The finite difference solutions for f_V were based on a leapfrog scheme in x with the Dufort-Frankel technique[13] applied to the second-order V derivative. Second-order differencing was applied throughout with the directional nature of the η derivative taken into account near the η boundaries of the computational domain. This finite difference scheme resulted in an explicit marching procedure used to advance the solution for f_V until it no longer varied with x. In addition to the boundary conditions, the calculation is subject to an integral constraint characteristic of pdf's.

$$\int_{-\infty}^{\infty} f_V\,dV \equiv 1 \tag{17}$$

Due to the preliminary nature of the calculations reported herein, little effort was directed toward optimizing the numerical scheme. As such, a uniform spacing of mesh points was used. It might be wise in future investigations to consider the advantages of a nonuniform grid or coordinate mapping. One of the uses of these initial solutions (to be discussed in the following section) is to provide guidance in the selection of just such improvements for use in future velocity space calculations.

Discussion of Results

In this section, solutions for f_V are presented and discussed for the two-dimensional turbulent shear layer geometry with comparisons made for the data of Spencer and Jones.[8] The detailed solutions in velocity space will be used to explain the structure of turbulent transport based on the statistical nonequilibrium of the velocity fluctuations. Finally, various moments of the solution will be formed according to Eq. (1) in order to investigate the mean behavior of the flowfield.

Velocity Space Structure of Solutions

The first element of the solutions to be discussed is a plot of $f_{\hat V}$ vs $\hat V$ at three locations in the mixing layer as shown in Fig. 3. Included are the data taken from Ref. 8. The choice of mesh points did not permit comparison at identical η locations. However, the present discussion is centered about the qualitative behavior of the solutions. The calculation displays Gaussian behavior on the dividing streamline and oppositely skewed forms at the two other locations. The data confirm this predicted behavior. A Gaussian distribution of velocity fluctuations has only nonzero even-order moments; thus the odd-order moments such as $\langle \hat V^3\rangle$ which govern transport are zero. This result corresponds with observations of the mean flow behavior for this geometry which show that

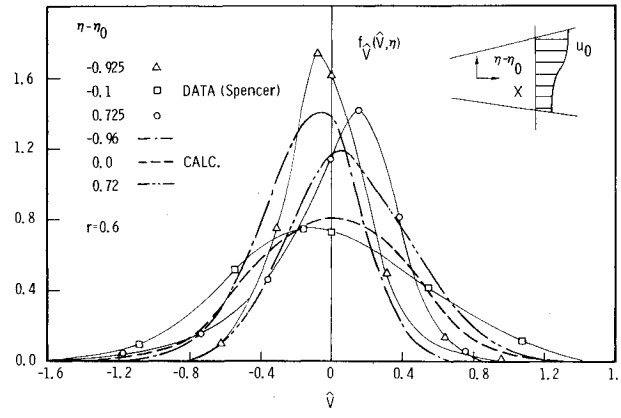

Fig. 3 Comparison of $f_{\hat V}$ solution with data of Spencer.

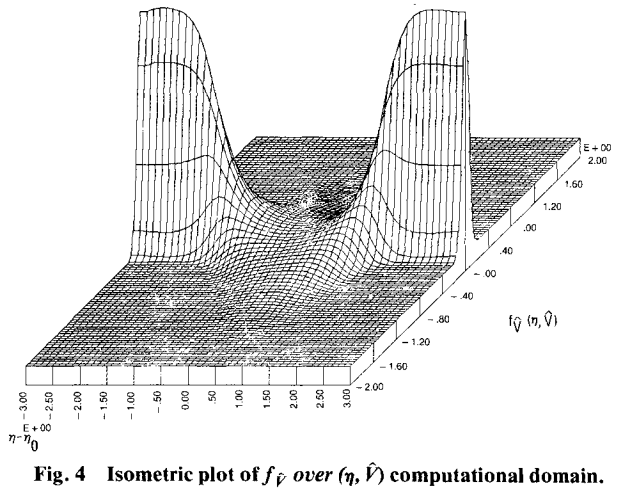

Fig. 4 Isometric plot of $f_{\hat V}$ over $(\eta, \hat V)$ computational domain.

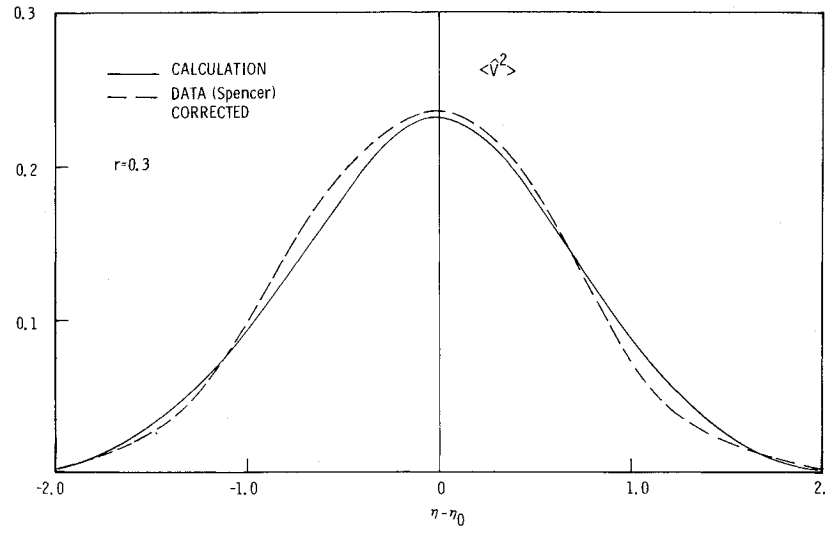

Fig. 5 Comparison of second moment of $f_{\hat{V}}$ solution with data of Spencer, $r = 0.3$.

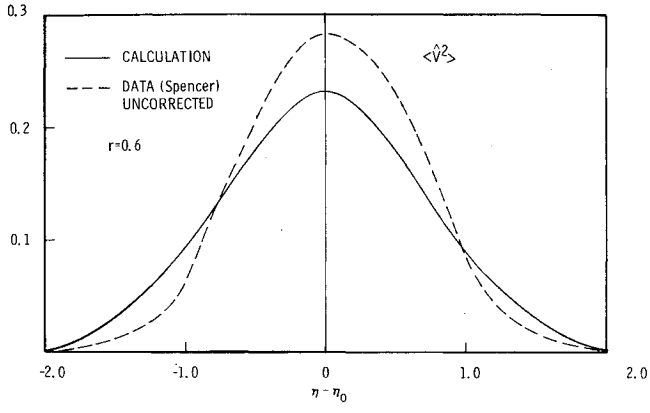

Fig. 6 $\langle \hat{V}^2 \rangle$ comparison for $r = 0.6$.

the turbulent transport of turbulent kinetic energy passes through zero in the vicinity of the dividing streamline. This occurrence generally corresponds to a maximum in the turbulence energy which is part of the basis for gradient diffusion models. The skewed velocity distributions of Fig. 3 possess nonzero odd-order moments and hence nonzero turbulent transport of $\langle \hat{V}^2 \rangle$. The opposite skew on the two sides of the dividing streamline imply oppositely directed transport, which also agrees with the known behavior of the mean flowfield. These solutions clearly demonstrate the relationship between turbulent transport and the statistical nonequilibrium of the velocity fluctuations.

Upon further inspection of the solutions of Fig. 3, it is noted that the velocity distribution is broad with a reduced peak at the dividing streamline while its form becomes narrow with a higher peak away from the dividing streamline. The correspondence between changes in the peak and the breadth are a result of the requirement that the pdf be normalized to one. This variation in the spread of f_V, because it is a measure of the second moment $\langle \hat{V}^2 \rangle$, implies the occurrence of the expected peak in turbulence energy in the central region of the shear layer and a falling off toward the edges. These basic features of the solution are summarized in the isometric plot of Fig. 4. Some study is required to identify the skew in this plot. However, the three-dimensional plot does provide a good visualization of the evolution of $f_{\hat{V}}$ from the low energy Gaussian function in one stream to the broad high-energy profile and back to the narrow Gaussian of the second stream as the mixing layer is traversed.

The behavior of $f_{\hat{V}}$ shown in Figs. 3 and 4 is easily related to the dynamics of $f_{\hat{V}}$ through Eq. (8). The skewed distribution observed on the interior of the mixing layer results from the warping effect of the η derivative under the action of the mean shear. This same term leads to the transport term involving $\langle \hat{V}^3 \rangle$ when the moment equation for $\langle \hat{V}^2 \rangle$ is derived from Eq. (8). This emphasizes intimate coupling in the statistical approach between the mean turbulent transport and the developing solution for $f_{\hat{V}}$. The height and breadth of $f_{\hat{V}}$ which governs $\langle \hat{V}^2 \rangle$ is strongly influenced by the competition between the first- and second-order $\hat{V}$ derivatives. The first-order derivative drives $f_{\hat{V}}$ toward a delta function of zero turbulence energy suggesting a dissipation mechanism, while the second-order term diffusively spreads $f_{\hat{V}}$. In the absence of mean shear or η gradients, these two mechanisms are balanced resulting in a Gaussian solution to Eq. (8). This is exactly the situation in the bounding streams at $\eta \to \pm\infty$. The interplay of these three mechanisms of dissipation, generation, and transport are governed by the geometry of the flowfield to determine the solutions of Fig. 3. That is, the ratio $3(1+D)/\langle U_k U_k \rangle$ governs the energy in the velocity fluctuations by adjusting the relation between the $\hat{V}$ derivatives. The term $B\epsilon^{1/2}$ governs the balance between this energy process and the spatial gradients in the flowfield imposed by the boundaries, thereby determining the state of statistical nonequilibrium which is the basis for the transport. With the turbulent structure explained on the basis of the statistical behavior of the fluctuating velocity field by means of the solutions for $f_{\hat{V}}$, attention will now be focused upon description of the mean two-dimensional shear layer behavior.

Mean Flowfield Structure

The calculated mean structure of the $\hat{V}$ component of the turbulence field is obtained from moments of the $f_{\hat{V}}$ solution as defined by Eq. (1). The calculation for $\langle \hat{V}^2 \rangle$ [$Q = \hat{V}^2$ in Eq. (1)] is compared with the data of Spencer and Jones[8] in Figs. 5 and 6 for velocity ratios of $r = 0.3$ and $r = 0.6$, respectively. There is general agreement between the data and the calculations. The asymmetry in the calculation, apparent to some degree in the data, can be traced to the coefficient of f_V in the first-order velocity derivative of Eq. (8).

The variation in agreement between Figs. 5 and 6 is of the same order as that found by other investigators when comparing the total turbulence energy results of separate experiments. Varma et al.[14] compare their calculations for peak total turbulence energy in the shear layer with data from various experiments. The compilation of data from that comparison shows no strong indication of a single trend of turbulence energy level with r. The calculations of Vollmer and Rotta[15] for the Spencer and Jones data actually displays the opposite variation of turbulence levels with r. The present analysis does not provide total turbulence energy profiles; however, it is concluded that the agreement for $\langle \hat{V}^2 \rangle$ is well within the bounds expected for free shear flows.

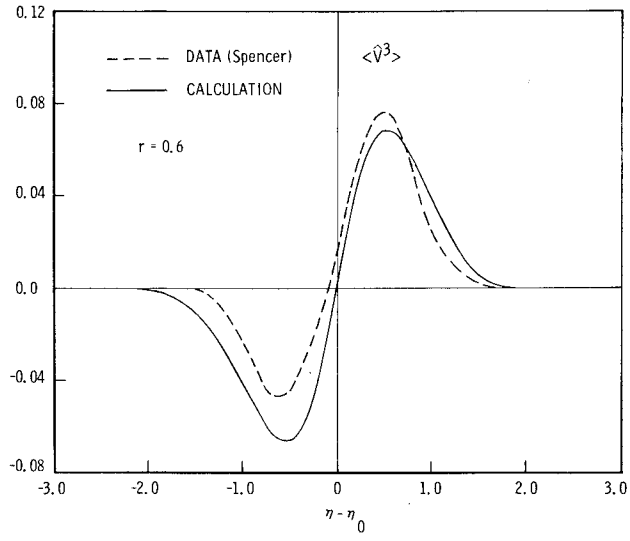

Fig. 7 Comparison for $\langle \hat{V}^3 \rangle$, $r=0.6$.

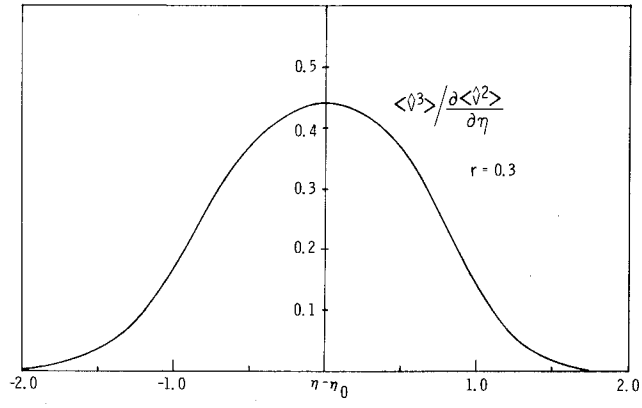

Fig. 8 Transport coefficient for $\langle \hat{V}^2 \rangle$ derived from $f_{\hat{V}}$ solution, $r=0.3$.

One further point of interest in considering the data of Spencer and Jones is that corrections were applied only to the $r=0.3$ data. It was pointed out that the corrections would not be as significant for the $r=0.6$ case. Although the total turbulence energy profiles were not greatly disturbed, the relative values of the $\langle U^2 \rangle$, $\langle V^2 \rangle$, and $\langle W^2 \rangle$ components for $r=0.3$ were significantly altered as compared to the $r=0.6$ data. The result is an apparent difference in the basic turbulent structure for the two values of r. The order of the correction is the same as the variation in agreement between the data and the calculation presented herein.

In Fig. 7 the third moment $\langle \hat{V}^3 \rangle$ of the solution for $f_{\hat{V}}$ is compared only with data for $r=0.6$ because the data for $r=0.3$ was not published. The antisymmetry of the data is displayed by the calculation showing good agreement with peak numerical values. There is a significant difference in the degree of asymmetry between calculation and experiment. A detailed discussion of this aspect will have to be delayed until solutions are presented for the complete turbulence structure since, as noted earlier, there are some uncertainties in the experimental trends of individual components vs total turbulence energy with r. However, it can be stated that the present model does reproduce the correct mean structure of the turbulent transport as determined by moments of the solution for f_V.

As a result of being able to calculate all of the higher order velocity correlations such as $\langle \hat{V}^3 \rangle$ from the single solution for $f_{\hat{V}}$, it is possible to actually predict the turbulent transport coefficient for $\langle \hat{V}^2 \rangle$ for this particular geometry. The concept of such a coefficient arises from the assumption that $\langle \hat{V}^3 \rangle$, which represents the transport of $\langle \hat{V}^2 \rangle$, is proportional to the gradient of $\langle \hat{V}^2 \rangle$.

$$\langle \hat{V}^3 \rangle \propto \frac{\partial \langle \hat{V}^2 \rangle}{\partial \eta} \tag{18}$$

This assumption is required in moment closure approaches when closing the equations at the $\langle \hat{V}^2 \rangle$ level because there is no equation for $\langle \hat{V}^3 \rangle$. The proportionality "constant" for relation (18) is the turbulent transport coefficient which generally depends upon local turbulent structure. Because both sides of the proportionality relation are available from the $f_{\hat{V}}$ solution, the ratio has been formed and plotted in Fig. 8 for the eddy diffusivity profile of $\langle \hat{V}^2 \rangle$ in the present shear layer. Inspection of Figs. 5 and 8 suggests that if an eddy diffusivity were to be used, it should be modeled as being proportional to $\langle \hat{V}^2 \rangle$ which is the current practice in second-order closure models.[14] The description of the mean flowfield for the present problem based on solutions for $f_{\hat{V}}$ is now complete and in good agreement with known data.

Concluding Remarks

Numerical solutions for the normal component of the turbulence velocity pdf have been presented for the two-dimensional free shear layer. No significant numerical difficulties were encountered once the velocity space character of the boundary conditions was properly specified. This was achieved by appealing to the analogy with the kinetic theory of gases. The behavior of Eq. (8), subject to these boundary conditions, revealed a character similar to a recirculating flow in the η-V plane.

These initial solutions for the pdf demonstrate the tractability of velocity space calculations. One drawback to the velocity space approach is the higher dimensionality of the added independent velocity variables. However, the reduction technique of partially integrating the equation for f attenuates this problem. The inception of advanced computers[16] and the storage and time savings of spectral computational techniques[17] may eventually deemphasize attempts at reducing dimensionality.

The comparisons presented for both the velocity space and the mean structure of the solution demonstrate good agreement with data. Beyond this result, the insight into turbulent structure available through the statistical approach has been further demonstrated with the velocity space solutions. Using the dynamics of f to look beyond correlations reveals the basis for transport in the statistical nonequilibrium of the velocity fluctuations which eliminates the need for empirical transport coefficients and intimately couples the transport mechanism with the evolving solution for f. The success of velocity space solutions to the present kinetic theory of turbulence in predicting two-dimensional shear layer characteristics suggests a new tool for the investigation of turbulence structure for engineering geometries.

In future studies attention will be directed toward removing the simplifications of supplying part of the mean flowfield which were introduced here to facilitate the demonstration of basic velocity space behavior at reduced computational effort. The same reduction technique of partially integrating over velocity space can be used for such calculations by developing additional equations from Eq. (5). The result will be no increase in the number of independent velocity space variables when calculating the complete turbulent structure for the present shear flow.

Acknowledgments

The author wishes to acknowledge the suggestions and criticism on the present work offered by Professor P. M. Chung of the University of Illinois, Chicago, Ill., and Drs. G. F. Widhopf, T. C. Lin, and J. W. Murdock of The Aerospace Corporation, El Segundo, Calif.

References

[1] Launder, B. E., Reece, G. J., and Rodi, W., "Progress in the Development of a Reynolds-Stress Turbulence Closure," *Journal of Fluid Mechanics,* Vol. 68, No. 3, 1975, pp. 537-566.

[2] Chung, P. M., "Turbulent Chemically Reacting Flows," Rept. No. TR-1001(S2855-20)-5, The Aerospace Corp., San Bernardino, Calif., 1967.

[3] Chung, P. M., "On the Development of Diffusion Flame in Homologous Turbulent Shear Flows," AIAA Paper 70-722, June 1970.

[4] Chung, P. M., "Turbulence Description of Couette Flow," *Physics of Fluids,* Vol. 16, July 1973, p. 880.

[5] Bywater, R. and Chung, P. M., "Turbulent Flow Fields with Two Dynamically Significant Scales," AIAA Paper 73-646, July 1973.

[6] Hong, Z. C., "Turbulent Chemically Reacting Flows According to a Kinetic Theory," Ph.D. Thesis, Dept. of Energy Engineering, Univ. of Illinois at Chicago Circle, Chicago, Ill., 1975.

[7] Huang, A. B., Hwang, P. F., Giddens, D. P., and Srinivasan, R., "High Speed Leading Edge Problem," *Physics of Fluids,* Vol. 16, No. 6, June 1973, p. 814.

[8] Spencer, B. W. and Jones, B. G., "Statistical Investigation of Pressure and Velocity Fields in the Turbulent Two-Stream Mixing Layer," AIAA Paper 71-613, June 1971.

[9] Chung, P. M., "A Kinetic-Theory Approach to Turbulent Chemically Reacting Flows," *Combustion Science and Technology,* Vol. 13, July 1976, pp. 123-153.

[10] Schlichting, H., *Boundary Layer Theory,* McGraw-Hill, New York, 1955.

[11] Hayday, A. A. and Chung, P. M., "On Turbulent Flow and Pumping in the Cavity of a Chemical Laser," *Second International Symposium on Gas-Flow and Chemical Lasers,* Von Karman Institute for Fluid Dynamics, Belgium, Sept. 1978.

[12] Anderson, D. G. M., "Plane Couette Flow and Heat Transfer with the Maxwell Boundary Condition," *Proceedings of the Sixth International Symposium on Rarefied Gas Dynamics,* Vol. 1, Academic Press, New York, July 1968, pp. 225-232.

[13] Roache, P. J., *Computational Fluid Dynamics,* Hermosa Publishers, Albuquerque, New Mex., 1972.

[14] Varma, A. K., et al., "Application of Invariant Second Order Closure Model to Compressible Turbulent Shear Layers," AIAA Paper 74-592, June 1974.

[15] Vollmers, H. and Rotta, J. C., "Similar Solutions for Turbulent Flows Described by Mean Velocity, Turbulent Energy, and Turbulent Length Scale," AIAA Paper 76-407, July 1976.

[16] Widhopf, G. F. and Taylor, T. D., "New Computer Technology and Potential Impacts on Fluid Dynamic and Atmospheric Pollution Studies," AIAA Paper 78-294, July 1978.

[17] Murdock, J. W., "A Numerical Study of Nonlinear Effects on Boundary Layer Stability," *AIAA Journal,* Vol. 15, Aug. 1977, pp. 1167-1173.